Phonon-limited performance of single-layer, single-gate black phosphorus n- and p-type field-effect transistors

Aron Szabo, Reto Rhyner, Hamilton Carrillo-Nunez, and Mathieu Luisier
Email: szaboa@iis.ee.ethz.ch, Phone: +41 44 632 5727, Fax: +41 44 632 1194, ETHZ, 8092 Zürich, Switzerland

***Abstract*— Phosphorene is a novel 2-D material with a direct band gap and a high electron/hole mobility, which makes it attractive for logic applications. The theoretical investigations of such devices have so far lacked either one or both key ingredients of realistic simulations: a full-band description of the electronic states and the consideration of electron-phonon scattering. In this paper we present the first *ab-initio* quantum transport simulations of phosphorene transistors accounting for these effects. We show that the DOS bottleneck does not limit the performance of phosphorene FETs, that the armchair configuration takes advantage of its lower effective mass and higher mobility at gate lengths above 10 nm, but that these properties become an obstacle at shorter gate lengths. We also demonstrate that phosphorene FETs with 10 nm gate length outperform MoS_2, regardless of the channel orientation.**

Introduction

Few-layer black phosphorus (phosphorene) has recently stood out from the 2-D crystal family as a promising field-effect transistor (FET) candidate at the end of the semiconductor roadmap. Besides the excellent electrostatic control inherent to the 2-D technology, black phosphorus exhibits a direct band gap and significantly higher mobility values than most transition metal dichalcogenides (TMDs), making it a strong competitor in the race for ultimate logic devices.

The demonstration of a high drain current modulation and high field-effect mobility [1] has aroused the interest of the scientific community for black phosphorus. Despite already spectacular achievements it remains to determine whether phosphorene is capable of outperforming ultra-scaled Si or TMD-based switches. To answer this question computer simulations can assist the on-going experimental efforts and shed light on the characteristics of not-yet-fabricated devices in a time- and cost-efficient way. So far phosphorene FETs have been simulated either within a simple Top-of-the-Barrier approach [2] or using a 4-band tight-binding model [3], in both cases in the ballistic limit of transport. The influence of electron-phonon scattering has also been investigated, but only with respect to the phonon-limited carrier mobility calculated with acoustic deformation potentials [4].

In this paper we go one step further and present the first *ab-initio* quantum transport simulations of single-layer phosphorene FETs including electron-phonon scattering (acoustic and optical). We confirm the strong anisotropy of their transport properties and establish that both the electron and hole mobilities are larger in the armchair (X) direction than in the zigzag one (Y), contrary to previous claims [4]. We show that transport along X is more favorable than along Y due to a lower effective mass and no density-of-states (DOS) bottleneck effects. However, the situation changes when the gate length scales below 10 nm. We lastly demonstrate that phosphorene outperforms MoS_2 at L_g=10 nm.

Approach

The same *ab-initio* scheme as in Refs. [5] and [6] is used to simulate black phosphorus samples. The Bloch-electron states of single-layer crystals are computed with the VASP density-functional theory (DFT) tool [7]. The GGA functional of Perdew-Burke-Ernzerhof is utilized because it implicitly accounts for the screening by the substrate through its known band gap underestimation. The phosphorene layer is separated from its periodic replica by a 20 Ångström vacuum region. A set of ionic relaxations are performed in fixed unit cells with various lattice vectors. The equilibrium lattice constants are determined as the minimum position of a quadratic fit to the total energies. A force of less than 10^{-3} eV/Å acting on each ion and a total energy difference smaller than 10^{-5} eV between two subsequent electronic steps are chosen as convergence criteria. A $15 \times 1 \times 15$ Monkhorst-Pack k-point grid and a 500 eV plane wave cutoff energy is applied in the geometric optimization process. Spin-orbit coupling is neglected. The lattice constants are found to be $a_x = 4.38$ Å and $a_y = 3.31$ Å. After determining the relaxed geometry the electron states are computed on a $21 \times 1 \times 21$ k-point grid using a 550 eV cutoff, yielding a direct gap of 0.91 eV at Γ.

The plane waves are then transformed into a set of maximally-localized Wannier functions (MLWFs) using the Wannier90 tool [8]. Four orbitals are considered on each of the four P atoms forming the unit cell giving rise to 10 valence and 6 conduction bands. Electron states within a 5 eV interval centered at the mid-gap energy are frozen when disentangling the subspace of the 16 Wannier functions from the higher energy bands [9]. The quadratic spread of each of the resulting MLWFs is less than 2 Å^2 so that the resulting Hamiltonian matrix displays a tight-binding-like sparsity pattern. Hopping terms are kept within a 18.5 Å interaction range, producing an excellent agreement with the DFT data, as demonstrated in Fig. 1. The generated Hamiltonian matrix is then loaded into a quantum transport solver based on the Non-equilibrium Green's Function (NEGF) method [10].

The dynamical matrix of phosphorene is also determined with VASP using density-functional perturbation theory (DFPT). The phonon modes and frequencies are extracted with the help of the Phonopy package [11] and are reported in Fig. 1(d). The electron-phonon coupling constants are computed by applying hydrostatic strain to the phosphorene

layer in VASP and transforming the difference of the perturbed and unperturbed Hamiltonian into the same MLWF basis [6]. With these data we are able to perform dissipative quantum transport simulations of nanoscale devices including electron-phonon scattering [12].

Results

Phosphorene FETs with a single-gate configuration (L_g=10.5 nm), as depicted in Fig. 1(b), are simulated with and without electron-phonon scattering. Their electron and phonon bandstructures are shown in Figs. 1(c-d), validating the MLWF approach. A 4-band tight-binding model as in Ref. [3] does not provide such a good reproduction of the DFT bandstructure.

First, the phonon-limited electron and hole mobility of single-layer black phosphorus is reported in Fig. 2. The linear dependence of the resistance on the channel length clearly demonstrates the diffusive nature of transport. The dR/dL method [13] is employed to compute the mobility of both carrier types, which exhibits a strong anisotropy: the value along X is larger than along Y, reaching 2500 cm^2/Vs for electrons and 3000 cm^2/Vs for holes. In Ref. [4] where a single-parameter deformation potential model was used to evaluate the phonon-limited carrier mobilities, a hole mobility 16-38 times larger in the Y direction than in the X one was predicted. Contrary to these claims, we find that even for holes the X direction gives a higher mobility, about 18 times larger than in the Y direction. For electrons the mobility in the X direction exceeds the one along Y by a factor of 4. Note that Ref. [4] reports a 14-fold improvement in favor of X, three times more than in our calculations.

Although electron-phonon scattering only slightly affects the spectral current of phosphorene FETs, as illustrated in Fig. 3(a), this effect is still included in the calculation of the $I_d - V_g$ of p- and n-type devices. The transfer characteristics at $V_{ds} = 0.67$ V are reported in Figs. 3(b-c). All the currents reach about 90% of their ballistic limit and significantly depend on the channel orientation, reflecting the anisotropy of the mobilities and effective masses: the ON-current is about three times larger in X-oriented p-FETs than in Y-oriented ones and it is more than twice higher in n-FETs with a channel direction along X than in transistors with transport along Y.

It is clear from Fig. 4 that the simulated FETs do not suffer from the DOS bottleneck effect at the selected EOT. The slope of the charge vs. gate voltage plot remains the same in each device, indicating that the gate capacitance is dominated by the oxide capacitance. As a consequence, the lower effective mass along X induces a higher carrier velocity and larger currents. This is an obvious advantage over III-V devices where the benefit of a high carrier velocity is partly annihilated by the reduced carrier population due to the isotropy of the electron bandstructure.

Small effective masses limit however the gate length scalability of black phosphorus transistors due to the increased source-to-drain tunneling leakage, as can be seen in Fig. 5. The sub-threshold slope of both n- and p-FETs deteriorates much faster if the channel is oriented along X, making such devices impractical at 5 nm gate lengths. However, a double-gate design, as investigated in Ref. [3] might help the X-oriented devices maintain their advantage even at this scale.

Finally, the performance of single-layer black phosphorus and MoS_2 FETs are compared to each other. For the phosphorene the Y channel orientation is chosen, due to its better scalability, while the transport properties of MoS_2 are isotropic. The carrier mobilities are shown in Fig. 5(c). In MoS_2 the hole mobility is larger than the electron mobility, the opposite of what is observed in phosphorene. The surprising feature of this plot is that the hole mobility along the Y-direction in phosphorene increases with the carrier concentration. This finding is attributed to the heavy non-parabolicity of the valence band along the Y direction. The $I-V$ characteristics are reported in Figs. 6(a-b). While the phosphorene FET with transport along X clearly outperforms the MoS_2, the difference is much smaller for the Y channel, especially in the p-type case. The most important device metrics that were calculated are summarized in Fig. 6(c).

Conclusion

Black phosphorus FETS have been simulated at the *ab-initio* level in the presence of electron-phonon scattering. The extracted mobility and current values indicate that this material holds great promise down to 10 nm gate lengths, but might lose its advantages over e. g. MoS_2 when further scaled.

Acknowledgment

This work was supported by Swiss National Science Foundation Grant No. PP00P2_159314 and by a grant from the Swiss National Supercomputing Centre (CSCS) under Project ID s579. We also acknowledge PRACE for awarding us access to Fermi at CINECA in Italy. Financial support from the EU FP7 project DEEPEN is also acknowledged.

References

[1] L. Li *et al.*, *Nat. Nano.*, vol. 9, no. 5, pp. 372–377, 2014.
[2] K.-T. Lam, Z. Dong, and J. Guo, *Electron Device Letters, IEEE*, vol. 35, no. 9, pp. 963–965, 2014.
[3] F. Liu, Y. Wang, X. Liu, J. Wang, and H. Guo, *Electron Devices, IEEE Transactions on*, vol. 61, no. 11, pp. 3871–3876, 2014.
[4] J. Qiao, X. Kong, Z.-X. Hu, F. Yang, and W. Ji, *Nat. Commun.*, vol. 5, p. 4475, 2014.
[5] A. Szabo, R. Rhyner, and M. Luisier, in *Electron Devices Meeting (IEDM), 2014 IEEE International*, 2014, p. 30.4.1.
[6] A. Szabó, R. Rhyner, and M. Luisier, *Phys. Rev. B*, vol. 92, p. 035435, 2015.
[7] G. Kresse and J. Furthmüller, *Phys. Rev. B*, vol. 54, p. 11169, 1996.
[8] A. A. Mostofi *et al.*, *Computer Physics Communications*, vol. 178, no. 9, pp. 685 – 699, 2008.
[9] I. Souza, N. Marzari, and D. Vanderbilt, *Phys. Rev. B*, vol. 65, p. 035109, 2001.
[10] M. Luisier, A. Schenk, W. Fichtner, and G. Klimeck, *Phys. Rev. B*, vol. 74, p. 205323, 2006.
[11] A. Togo, F. Oba, and I. Tanaka, *Phys. Rev. B*, vol. 78, p. 134106, 2008.
[12] M. Luisier and G. Klimeck, *Phys. Rev. B*, vol. 80, p. 155430, 2009.
[13] K. Rim, S. Narasimha, M. Longstreet, A. Mocuta, and J. Cai, in *Electron Devices Meeting, 2002. IEDM '02. International*, 2002, pp. 43–46.

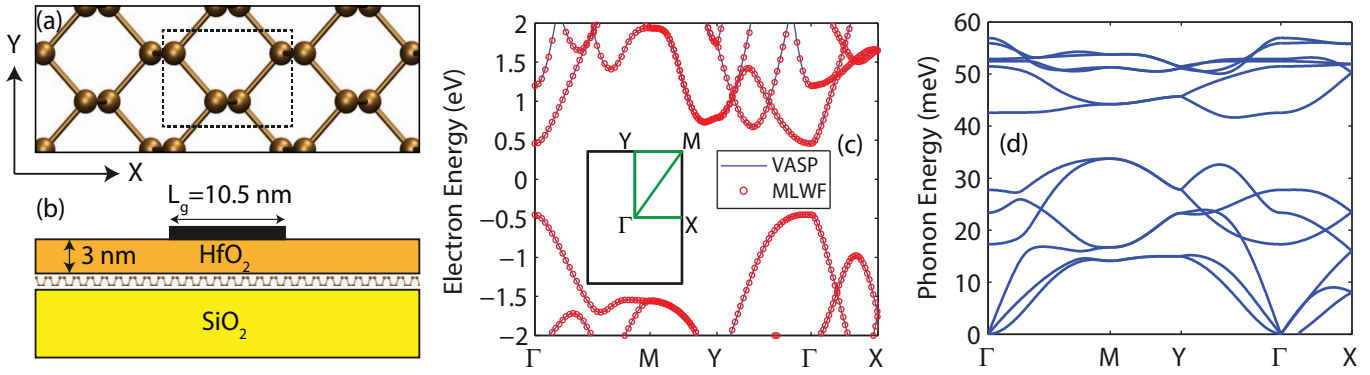

Fig. 1. (a) Top view of the atomic structure of single-layer black phosphorus. The X and Y crystal orientations are indicated with arrows. (b) Schematic view of the single-layer, single-gate n- and p-type black phosphorus field-effect transistors considered in this work. The gate length is originally set to L_g=10.5 nm while the source and drain regions extend over L_s=L_d=15 nm and are doped with a donor (acceptor) concentration N_D=4e13 cm^{-2} (N_A=4e13 cm^{-2}) in the n-type (p-type) configuration. The equivalent oxide thickness of all the transistors is equal to EOT=0.58 nm (3 nm of HfO_2 with ϵ_R=20). The phosphorene channels are deposited on a 20 nm SiO_2 substrate. The out-of-plane direction is modeled with 21 k-points. All the simulations are performed at room temperature. (c) Single-layer black phosphorus electronic bandstructure as calculated with the VASP tool (blue lines) and as obtained after a transformation into the maximally localized Wannier function basis used in quantum transport simulations (red circles). (d) Phonon bandstructure of single-layer black phosphorus as calculated with VASP.

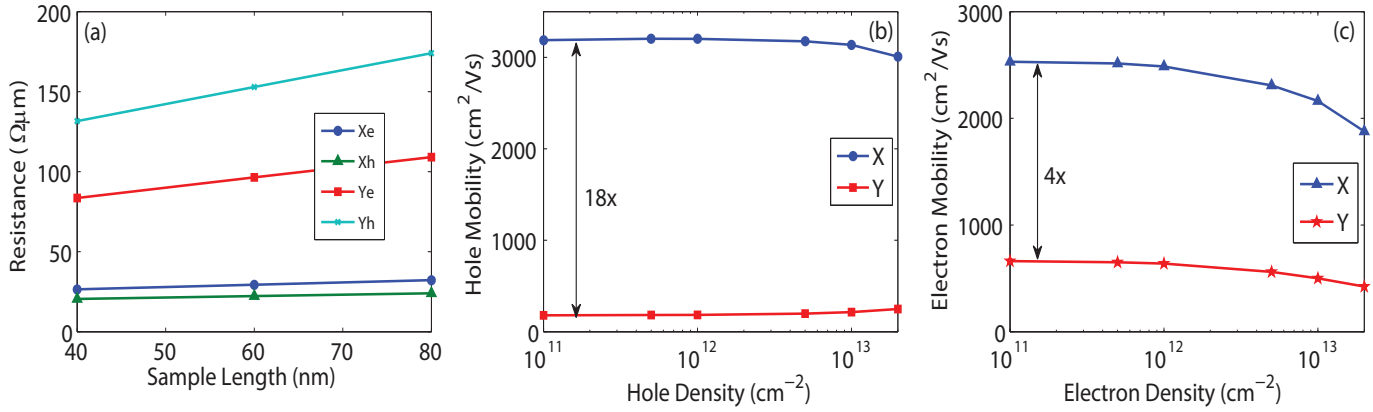

Fig. 2. (a) Channel resistance of n- and p-type single-layer black phosphorus samples as a function of their length (40, 60, and 80 nm) and their transport direction (X and Y). The charge concentration is equal to 2e13 cm^{-2} in all cases. As expected with diffusive transport, the resistance linearly increases with the sample length. (b) Phonon-limited hole mobility of monolayer black phosphorus as a function of the hole concentration (1e11$\leq p_{2D} \leq$ 2e13 cm^{-2}) and transport direction (X: blue line with circles, Y: red line with squares). (c) Phonon-limited electron mobility of single-layer black phosphorus under the same conditions as in (b). Note that the omission of charged impurity scattering may explain why the calculated mobility values are higher than in experiments.

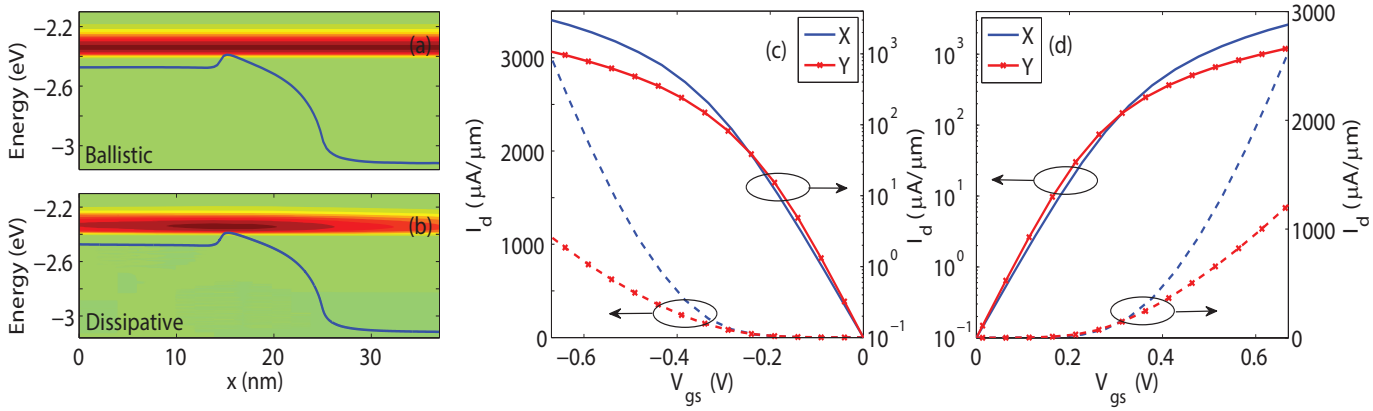

Fig. 3. (a) Ballistic spectral current (current as a function of the position and energy) flowing through a n-type black phosphorus FET with the same dimensions as in Fig. 1 and transport along Y. Red indicates high current concentrations, green no current. The blue line refers to the conduction band edge. (b) Same as in (a), but in the presence of electron-phonon scattering. Interactions with phonons have little influence on the current spectral distribution and on the profile of the conduction band. (c) Transfer characteristics I_d-V_{gs} at V_{ds}=0.67 V through a p-type single-layer, single-gate black phosphorus FET as in Fig. 1. Transport along the X (blue lines) and Y (red lines) crystal orientations is considered. A linear and logarithmic scale of the current are provided. (d) Same as (c), but for the n-type component.

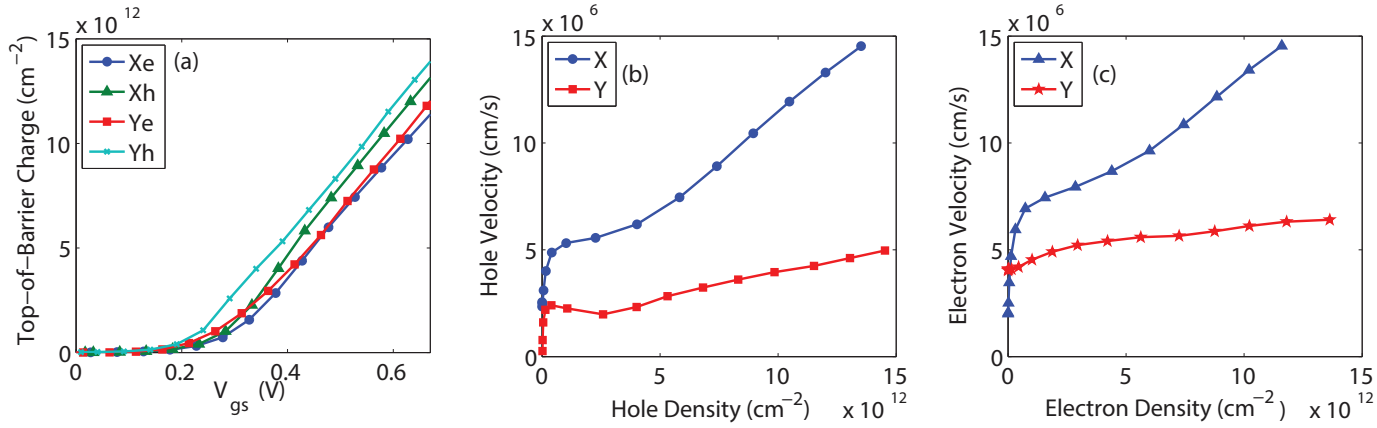

Fig. 4. (a) Charge concentration at the top of the potential barrier (ToB) separating the source and drain extensions of the 4 different single-layer, single-gate black phosphorus FETs investigated in this work (n- and p-type with transport along the X or Y crystal axis). The charge is reported with respect to the applied V_{gs} at V_{ds}=0.67 V. (b) Hole injection velocity extracted from the same p-type FETs as in (a) as a function of the hole concentration at the ToB and channel orientation (X: blue line, Y: red line). (c) Same as (b), but for the electron injection velocity. Electron-phonon scattering is included in all the cases.

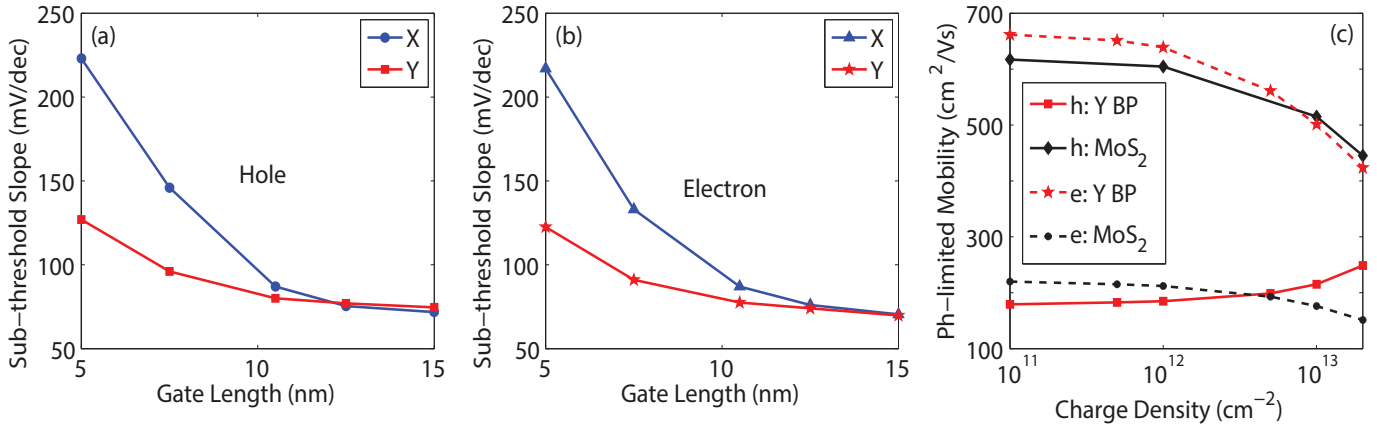

Fig. 5. (a) Sub-threshold slope (SS) of the p-type single-layer, single-gate black phosphorus FET shown in Fig. 1 as a function of its gate length (L_g=5, 7.5, 10.5, 12.5 and 15 nm) and channel orientation (X: blue line, Y: red line). SS is extracted at V_{ds}=0.67 V. (b) Same as in (a), but for the n-type FET. (c) Comparison between the phonon-limited electron and hole mobility of single-layer MoS_2 (black lines) and black phosphorus with transport along Y (red lines) as a function of the charge concentration.

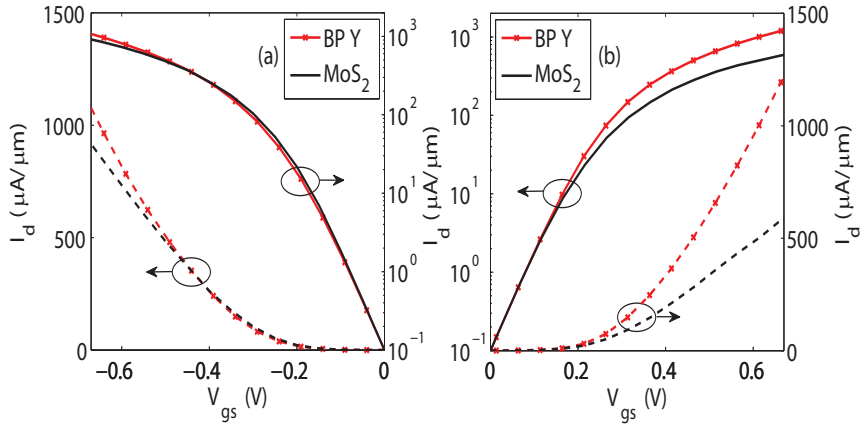

(c)

		nFET	pFET
X	I_{ON} ($\mu A/\mu m$)	2624	2995
	I_{OFF} ($\mu A/\mu m$)	0.1	0.1
	SS (mV/dec)	87	87
	Ballisticity (%)	93	95
	m^*_{trans} (m_0)	0.14	0.13
Y	I_{ON} ($\mu A/\mu m$)	1220	1077
	I_{OFF} ($\mu A/\mu m$)	0.1	0.1
	SS (mV/dec)	77.5	80
	Ballisticity (%)	88	89
	m^*_{trans} (m_0)	1.26	6.7

Fig. 6. (a) Comparison between the transfer characteristics of single-layer, single-gate MoS_2 (black lines) and Y-oriented black phosphorus (red lines) p-type FETs at V_{ds}=0.67 V. Both transistors have the same EOT=0.58 nm, gate length L_g=10.5 nm, and OFF-current I_{OFF}=0.1 $\mu A/\mu m$. (b) Same as in (a), but for the n-type FET. (c) Summary of the ON-current (I_{ON}), OFF-current (I_{OFF}), sub-threshold slope (SS), ballisticity of the ON-current, and transport effective mass (m^*_{trans}) for the 4 single-layer, single-gate black-phosphorus FETs simulated here. The gate length is set to L_g=10.5 nm and all the data are extracted at V_{ds}=0.67 V.